Nature and Science of Sleep

Elevate Series

Open Access Full Text Article

ORIGINAL RESEARCH

Bimodal Patterns of Locomotor Activity and Sleep in *Drosophila*: A Model for Their Simulation

Arcady A Putilov[1,*], Evgeniy G Verevkin[1,*], Dmitrii V Petrovskii[2,*], Lyudmila P Zakharenko[2,*]

[1]Independent Research Group "biomedical Systems Math-Modeling", Berlin, 12489, Germany; [2]Department of Insect Genetics, Institute of Cytology and Genetics of the Siberian Branch, the Russian Academy of Sciences, Novosibirsk, 630090, Russia

*These authors contributed equally to this work

Correspondence: Arcady A Putilov, Independent Research Group "Biomedical Systems Math-Modeling, 11, Nipkowstr, Berlin, 12489, Germany, Tel/Fax +0049-30-53674643, Email arcady.putilov@gmail.com

Purpose: Two previously proposed modelling approaches to explain the bimodal pattern of activity and/or sleep in *Drosophila melanogaster* are based on 1) the concept of morning and evening oscillators underlying the peaks of activity in the morning and evening, respectively, and 2) the concept of two cycles of buildup and decay of sleep pressure, gated only by the circadian oscillator. Previously, we simulated 24-h alertness–sleepiness curves in humans using a model postulating the circadian modulation of the buildup and decay phases of two (wake and sleep) homeostatic processes. Here, we tested whether a similar model could be applied to simulate the bimodal 24-h rhythm of fly locomotor activity and sleep.

Methods: To obtain typical curves for the simulations, a sample of 4263 individual 24-h curves of locomotor activity and sleep were subjected to principal component analysis. It yielded three principal components, which explained more than 70% of the individual variations in these curves. We calculated the typical curves using scores on the 1st, 2nd, and 3rd principal components and simulated these curves and the sample-averaged curves.

Results: We found that these curves are always characterized by two peaks with varying sizes and timings. They can be fitted by proposing the variation of some of the parameters of the two homeostatic processes reflecting the 24-h rhythmicity of the drive for wake and the 12-h rhythmicity of the drive for sleep.

Conclusion: Postulation of two separate circadian oscillators is not necessary to explain the bimodal curves in *Drosophila melanogaster*.

Plain language summary: This study tested whether a model postulating circadian modulation of the buildup and decay phases of two homeostatic processes (wake and sleep) can be applied to simulate the bimodal 24-h rhythm of fruit fly activity and sleep. The simulations suggested that the typical bimodal curves can be simulated by proposing variation of some of the parameters of the two underlying homeostatic processes that represent the 24-h variation in the drive for wakefulness and the 12-h variation in the opposing drive for sleep.

Keywords: sleep–wake regulating process, bimodal 24-h rhythm, fruit fly, math-modelling

Introduction

Many species of animals display a bimodal peak in their activity, that is, they show one peak in the morning and another peak in the evening (Aschoff, 1966).[1] *Drosophila melanogaster*, the main animal model for the basic research of the circadian rhythms and sleep, belongs to these species with bimodal activity. Under laboratory conditions, the fruit fly displays two activity peaks, one in the morning and one in the evening. A waveform of behavioral rhythms with two peaks is very different from the sinusoidal oscillations observed in clock genes. Therefore, the mechanisms in addition to the clock can have profound effects on their production (Lazopulo, Syed, 2017).[2]

The attempts to provide a model-based explanation of bimodal patterns of activity can be traced back to the 1970s when Pittendrigh and Daan (1976)[3] proposed a responsibility of two circadian oscillators, morning and evening, for the peaks of activity in the morning and evening, respectively. Indeed, the specialized morning and evening neurons have

Received: 23 September 2024
Accepted: 13 January 2025
Published: 18 January 2025

been later discovered in the fly's brain. However, some of such findings do not fit Pittendrigh and Daan's[3] model (Peschel, Helfrich-Förster, 2011; Menegazzi et al, 2020).[4,5] For instance, Grima et al (2023)[6] studied the rhythmic patterns of expression of the clock protein PERIOD (PER) in subsets of these morning and evening neurons and found that the expression in these neurons might peak more or less at the same time instead of showing the expected 8–10-h differences between the peaks of their activity. A study of rhythmic patterns of PER expression in subsets of morning and evening neurons in the fly's brain (Menegazzi et al, 2020)[5] led to the conclusion that the original dual oscillator model (Pittendrigh, Daan, 1976)[3] seems to be too simple to describe these patterns. The study suggested (Menegazzi et al, 2020)[5] that the circadian clock of this species is composed of a plastic network of numerous oscillators that rearrange themselves depending on environmental demands. Given such a complexity of the brain mechanism underlying the two peaks of activity, an explanation of the fly behavioral rhythms might require a more complex oscillatory model. For instance, Yoshii et al (2023)[7] recently proposed a model with four oscillators (two activity and two sleep oscillators) that reside in different clock neurons and regulate activity in the morning and evening, and sleep during midday and at night.

However, an alternative, more parsimonious (eg, one-oscillator) approach to model-based explanation of bimodality of fruit fly's rhythms was also proposed in the recent years. Abhilash and Shafer (2024)[8] applied the classical version of the two-process model of regulation of the human sleep–wake cycle to simulate the bimodal 24-h rhythm of *Drosophila* sleep. This two-process model postulates two – circadian and homeostatic – regulatory processes (Borbély, 1982; Daan et al, 1984)[9,10] and was initially introduced to explain the origin of the mostly unimodal 24-h cyclicity of human sleep and wakefulness. In the two-process model, this cyclicity is described as an inverse exponential buildup (1a) and an exponential decay of the homeostatic process (1b) during wakefulness and sleep, respectively, which is gated by the circadian process (ie, the gating occurs in such a way that the period of the homeostatic process normally remains equal to 24 h). Narrowing this circadian gate might be a parsimonious explanation for the transition of the unimodal pattern in humans to a bimodal pattern in *Drosophila melanogaster* (Abhilash, Shafer, 2024; Skeldon, Dijk, 2024).[8,11] Abhilash and Shafer (2024)[8] adapted Daan et al's (1984)[10] model for simulation of two peaks of fly's sleep by fitting homeostatic time constants so that sleep is biphasic and the percentage of sleep across the day matches the *Drosophila* pattern observed in the presence of a light–dark (LD) cycle.

However, the conceptualization and measurement of *Drosophila* sleep differ drastically from the conceptualization and measurement of human sleep. In accordance with the Donelson et al (2012)[12] criterion, fly sleep is conventionally defined as 5 consecutive minutes of the absence of any locomotor activity. Consequently, this is nothing more than another measure of locomotor activity. The classical two-process model can also be applied to simulate similar human 24-h rhythms, such as the rhythm of alertness–sleepiness and the rhythm of performance. However, any of such attempts had always led to the incorporation of an additional (3rd) process in these models to better fit the alertness-sleepiness and performance rhythms. In the proposed models, this 3rd process was associated with sleep inertia (Achermann, Borbély, 1994; Akerstedt, Folkard, 1997),[13,14] the circadian sensitivity modulator (Jewett et al, 1999),[15] the wake-promoting brain areas competing with the sleep-promoting areas (Phillips et al, 2013),[16] and the drive for wake opposing to the drive for sleep (Putilov et al, 2014, 2015).[17,18]

Similar complication of the model can be expected from the attempts to fit the fly's locomotion pattern with simple exponential functions that showed that quantification of the main features of the fly's locomotion pattern can be achieved by fitting data with a model consisting of at least four exponential terms (Lazopulo, Syed, 2017).[2] In other words, not one pair but two different pairs of inverse exponential buildups (1a) and exponential decays (1b) are necessary to postulate for simulation of this pattern.

Consequently, the question arises of whether a model with at least three regulatory processes and/or four exponential terms can be applied to explain the mechanism underlying the bimodal rhythm of the fly. To our knowledge, such a model has not been previously implicated in modelling and simulation of the oscillatory mechanism underlying the biphasic 24-h pattern of locomotor activity and sleep in *Drosophila*.

For the present model-based simulations, we used a sample of 4263 pairs of individual 24-h curves of locomotor activity and sleep collected for four previous publications (Zakharenko, 2018, 2021, 2023, 2024).[19–22] The whole set of individual curves was subjected to principal component analysis to reveal the most important dimensions of individual variation in these curves. Scoring on three principal components yielded the most typical 24-h curves of locomotor

activity and sleep. They were simulated to test our hypothesis that a slightly modified model of human alertness–sleepiness rhythm can be applied to explain three basic regulatory processes producing these curves.

Materials and Methods

Sampling the Individual 24-h Patterns of Activity and Sleep

The sample of 4263 individual 24-h curves of locomotor activity and sleep included 12 datasets that were described in detail in four previous publications (Zakharenko, 2018, 2021, 2023, 2024).[19–22] The sample-averaged curves of locomotor activity and sleep are shown in Figures 1 and S1. The major characteristics of the datasets are listed in Tables S1 and S2, and some of the major results of their separate (12) analyses are summarized in Tables S3-S5 and Figures S2-S5.

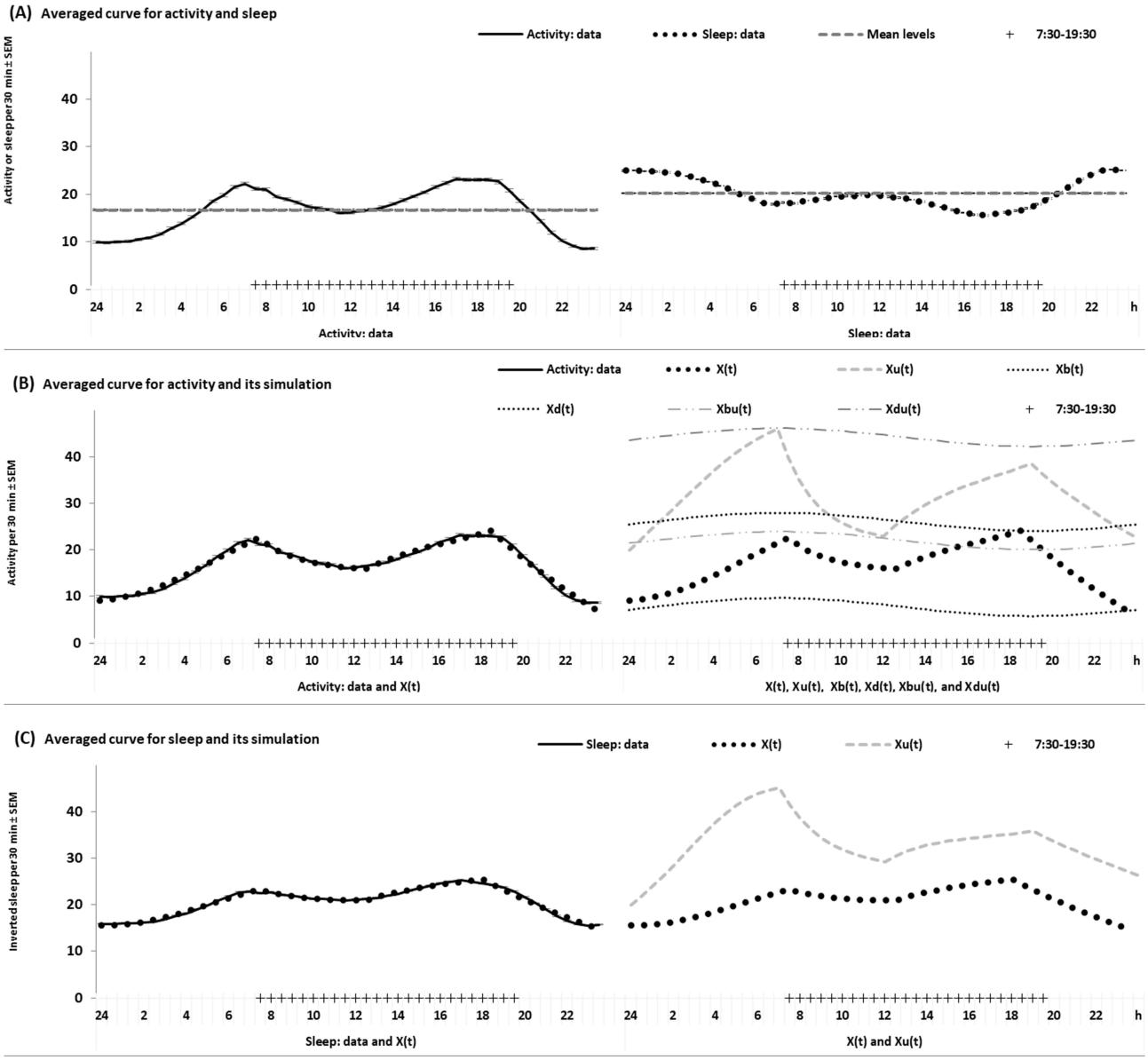

Figure 1 Averaged curves and their simulations. (**A**) The 24-h curves of locomotor activity (left) and sleep (right) obtained by averaging over 4263 individual curves from Datasets 1–12 (see Tables S1 and S2). (**B**) and (**C**) Simulation of the 24-h curve of locomotor activity and the 24-h curve of sleep, respectively (sleep curve inverted for simulation). Left: 24-h curve and its simulation, $X(t)$. Right: $X(t)$ and 5 separate parameters of the model, $X_u(t)$, $X_b(t)$, $X_d(t)$, $X_{bu}(t)$, and $X_{du}(t)$;. See Tables 2 and 3 and Figure S1 for parameter names; 7:30–19:30: Photoperiod during equinoxes in Novosibirsk.

https://doi.org/10.2147/NSS.S497563

Prior to recording locomotor activity, groups of 20–25 male or female flies from the same strain or cross were kept in standard vials under standard temperature (20°C) and either a standard 12-h photoperiod (light between 7:00 and 19:00) or a near-natural photoperiod established from the windows of a laboratory room in the absence of additional artificial illumination (light between 7:30 and 19:30 during equinoxes). To avoid the masking effects of light, darkness, and transitions between them, a vast majority of the records were obtained under constant darkness. Activity and sleep of flies were monitored and analyzed using a DAMS (Drosophila Activity Monitoring System; "Trikinetics", Waltham, MA, USA) and its software package (www.trikinetics.com, accessed on May 12, 2024). This system recognizes when an active fly is crossing the center of the locomotor tube, ie, by breaking the infrared beam passing across the middle of the tube (Pfeiffenberger et al, 2010).[23] Each fly was individually placed in the glass locomotor-monitoring tube of the DAMS with infrared beams for activity detection. The monitor was connected to a computer to record beam breaks at 1-min intervals. Locomotor activity was recorded after releasing the flies in constant darkness (DD) for at least 5 days. It was initially expressed as the number of beam breaks in 1-min bins, and these initial counts of locomotor activity were then used to quantify sleep events. In accordance with the Donelson et al (2012)[12] criterion, sleep was conventionally defined as 5 consecutive minutes of the absence of any locomotor activity.

Based on this approach to recording and calculating locomotor activity and sleep (www.trikinetics.com, accessed on May 12, 2024), Excel software was developed for further conventional analysis of locomotor activity and sleep over longer (30-min) intervals. The 1-min data were averaged over 30-min intervals for each record. Data for the first day were excluded as they mainly reflected the habituation process, whereas the following 30-min estimates of locomotor activity and sleep were averaged over four 24-h intervals to obtain measurements for each of the 48 time points constituting the 24-h cycle of an individual fly. These pairs of 48 values of the 24-h curves of 4263 individual flies (for locomotor activity and sleep) were subjected to statistical analysis. The Statistical Package for the Social Sciences ($SPSS_{23}$, IBM, Armonk, NY, USA) was used for statistical analysis. Some of the particular statistical results are included in Tables S3-S5, and the group-averaged results are illustrated in Figures 1–4 and S1 and S2.

Principal Component Scoring of the 24-h Individual Patterns

The two 24-h (48-time points) curves were obtained by averaging over all individual curves of locomotor activity and sleep (Figure 1A). To reveal the most important dimensions of individual variation in the 24-h curves, the whole sample of individual 24-h (48-time points) curves of locomotor activity or sleep was subjected to principal component analysis. It yielded three principal components explaining >70% of the total variation in the individual 24-h curves (Table 1, upper part). Loadings on these three components (Figure 2A) were used to calculate the typical curves for the pairs of subsamples with positive and negative scores (Figure 2B-D and Table 1). This allowed the reduction of the huge number of individual curves to a small number of most typical curves shown in Figure 2B-D. In Table 1, their main characteristics are compared with the characteristics of the sample-averaged curve.

Supplementary Material includes the results of additional statistical analyses of the 24-h curves in 12 separate datasets constituting the whole sample of 4263 individual curves of locomotor activity and sleep (Tables S3-S5 and Figure S2-S5). Details on the repeated-measures ANOVA (rANOVA) of the 24-h (48 time point) curves and principal component scores (the 1^{st}, 2^{nd} and 3^{rd}) are provided in Tables S3 and S4 (middle and right columns, respectively).

Model and Previous Simulations

Model-based simulations were performed using a model that was initially applied to simulate the 24-h patterns of alertness and sleepiness in humans (Putilov et al, 2014, 2015).[17,18] This model originates from a modification of the classical two-process model of sleep–wake regulation (Borbély, 1982; Daan et al, 1984)[8,9] that proposes the circadian modulation of the parameters of the homeostatic process underlying an overt circadian rhythm. Such modulation is incorporated into the model in the form of a very simple (sine) function (Putilov, 1995).[24] In its mathematical formulation, the homeostatic sleep process is identical to that of the classical two-process model of sleep–wake regulation (Borbély, 1982; Daan et al, 1984).[9,10] However, it has been additionally postulated that a very similar homeostatic process can underlie not only sleep homeostasis (Putilov, 1995)[23] but also wake (alertness–sleepiness) homeostasis (Putilov et al, 2014, 2015).[17,18]

Table 1 Three Principal Components and Features of Seven Curves of Locomotor Activity

Principal Component (PC)		**1st**		**2nd**		**3rd**	
Behavioral Measure		**Activity**	**Sleep**	**Activity**	**Sleep**	**Activity**	**Sleep**
Eigenvalue		25.96	22.78	7.16	7.56	2.78	3.54
% of Variance		54.09	47.45	14.92	15.75	5.78	5.78
Cumulative %		54.09	47.45	69.00	63.21	74.79	70.58
Activity curve	Averaged	1st PC score		2nd PC score		3rd PC score	
Main feature		+ (>0)	- (≤0)	+ (>0)	- (≤0)	+ (>0)	- (≤0)
Mean level	Middle	Higher	Lower	Middle	Middle	Middle	Middle
Amplitude	Middle	Larger	Smaller	Smaller	Larger	Larger	Smaller
Morning peak	7:00	7:00	7:00	6:30	7:00	6:30	7:00
Evening peak	18:30	18:30	18:30	19:00	16:30	19:00	16:30
Larger peak	None	None	Evening	Evening	Evening	Evening	Morning
Afternoon dip	Middle	Larger	Smaller	Larger	Middle	Middle	Smaller

Notes: Upper part. Three principal components were identified using principal component analysis of the individual curves for locomotor activity (activity) or sleep. Lower part: average locomotor activity curve was obtained by averaging the individual locomotor activity curves (n=4263). Six additional 24-h locomotor activity curves were calculated for subsamples with dichotomized scores on the 1st, 2nd and 3rd principal component (PC). Score + or Score –: positive and negative PC scores (above, below, or equal to zero, respectively). Main feature: a unique combination of the main features of a curve (compared to the averaged curve). The averaged curve is shown in in Figure 1A, the loading on three PCs is shown in Figure 2A, the curves for the dichotomized PC scores are shown in Figure 2B–2D, and the simulations of the seven curves are shown in Figure 1B, 3A-3C, and S1.

Therefore, the model includes two major homeostatic components, the representatives of the drive for sleep and the opposing drive for wakefulness. Additionally, the circadian component plays a role of modulator of the parameters of each of these two components. The model describes the homeostatic components as the alternations of an inverse exponential buildup with an exponential decay, eg, (1a) with (1b), respectively, for the wake (alertness-regulating) process, while the modulating circadian component of this or sleep-regulating process is represented by a sine function, eg, (2).

If t_1 and t_2 are the initial time points for the (inverse exponential) buildup and (exponential) decline phases of the wake process, the following formulae describe two (daytime and nighttime) parts of the 24-h fluctuations in the alertness–sleepiness level:

$$X(t) = [X_u + C(t)] - \{[X_u + C(t)] - X_b\} * e^{-(t-t1)/[Tb-k*C(t)],} \quad (1a)$$

$$X(t) = [X_l + C(t)] - \{X_d - [X_l + C(t)]\} * e^{-(t-t2)/[Td-k*C(t)]} \quad (1b)$$

where

$$C(t) = A * sin(2\pi * t/24 + \varphi_0) \quad (2)$$

is a periodic function with a 24-h period (Putilov, 1995; Putilov et al, 2014, 2015).[17,18,24]

Because alertness demonstrates a gradual declining trend from one day to another in the course of prolonged wakefulness, such an impact of another homeostatic process, sleep homeostasis, is incorporated in the model in the form of variation in an upper asymptote, X_u, of $X(t)$. It is assumed that this asymptote cannot remain constant throughout the buildup and decay phases of the alertness–sleepiness rhythm, as described in Equation (1a). Instead, it exhibits decay and buildup owing to the influence of the sleep homeostatic process, $X_u(t)$. For instance,

https://doi.org/10.2147/NSS.S497563

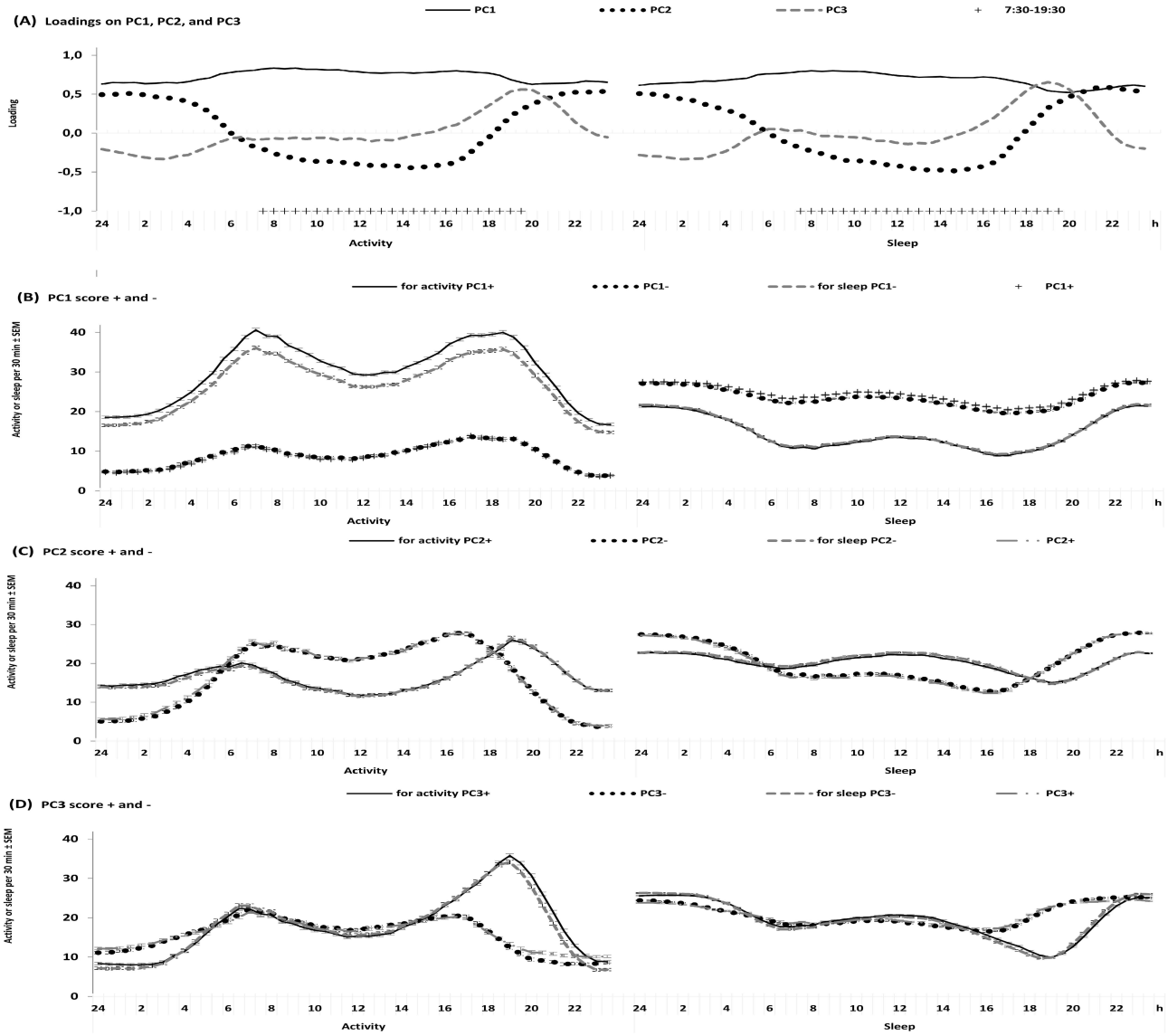

Figure 2 Curves calculated for subsamples with high and low principal component scores. (**A**) Loadings of the 30-min values of locomotor activity (left) and sleep (right) on the 1st, 2nd and 3rd principal components. (**B**–**D**) The 24-h curves of locomotor activity (left) and sleep (right) obtained for subsamples with dichotomized scores (above and below zero) on the 1st, 2nd and 3rd principal components. See also Table 1.

$$X_u(t) = [X_{lu} + C(t)] - \left\{X_{u1} - [X_{lu} + C(t)] * e^{-(t-t1)/[T_{du} - k*C(t)]}\right\}, \tag{3a}$$

where X_{u1} is the value of X_u at the initial time point t_1, and X_{lu} and T_{du} are the asymptote and time constants, respectively, of the decaying upper asymptote $X_u(t)$

In other words, this model interprets the process X(t) as an alternative homeostatic process representing the drive for wakefulness (ie, the wake-promoting process regulating the alertness–sleepiness rhythm). In contrast, the process $X_u(t)$ is interpreted as the representative of the opposing drive for sleep (ie, the sleep-promoting process associated with accumulation of sleep pressure during wakefulness and its dissipation during sleep, ie, this is, in fact, the classical homeostatic process in the Daan et al, 1984,[10] model. This interpretation corroborates the conceptualization of opponent drives for wake and sleep proposed by Edgar et al (1993)[25] and Dijk & Czeisler (1995).[26]

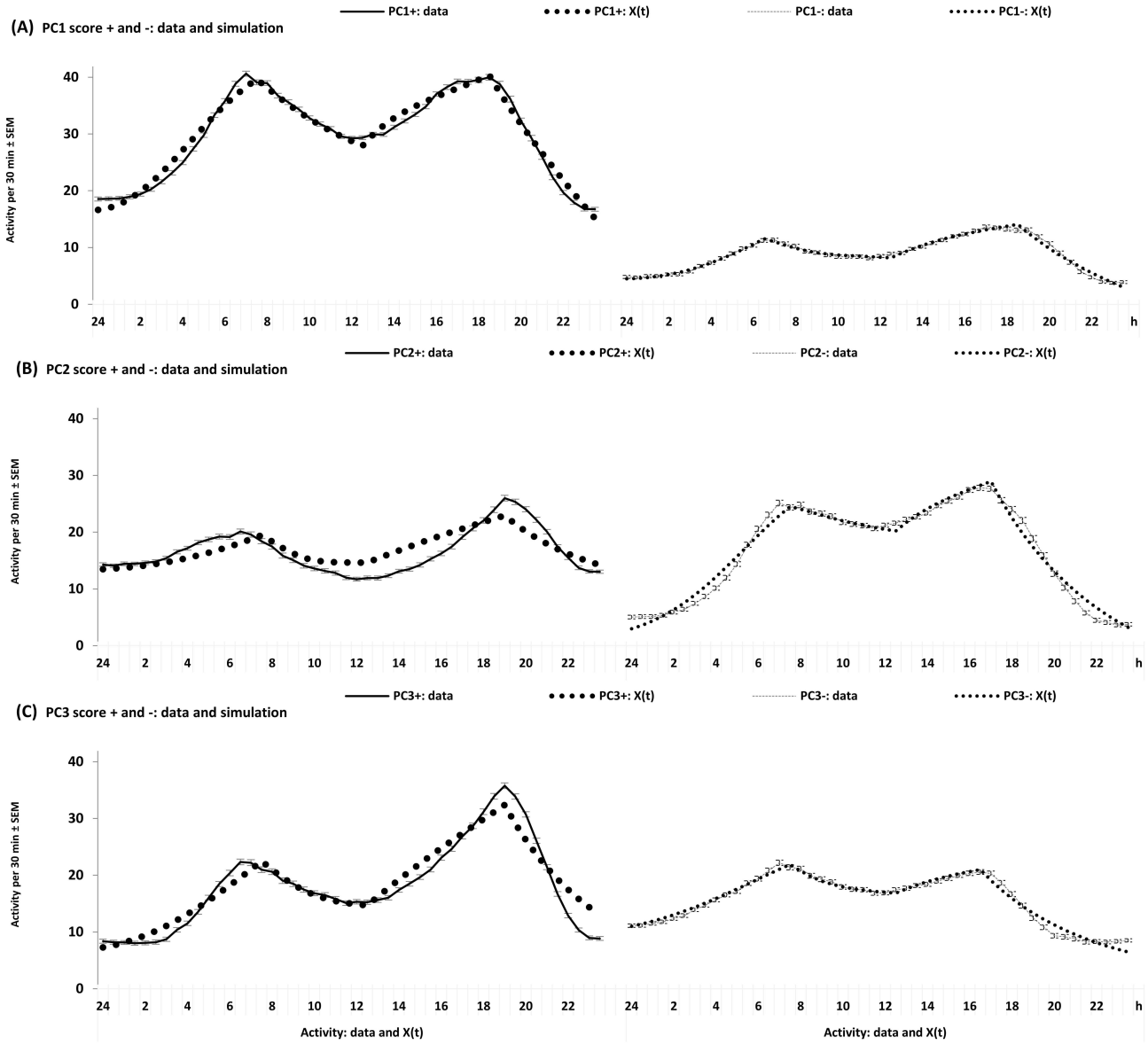

Figure 3 Simulations of activity curves for subsamples with different principal component scores. (**A**–**C**) The 24-h curves of locomotor activity for subsamples with the dichotomized scores (above and below zero) on the 1st, 2nd, and 3rd principal components, respectively, and their simulations, *X(t)*. Left and right: 24-h curves for scores above and below zero, respectively.

Present Simulations of the 24-h Individual Patterns

The only difference between the aforementioned model of the 24-h human alertness–sleepiness rhythm (Putilov et al, 2014, 2015)[17,18] and the model applied for the present simulations of the 24-h *Drosophila* rhythm was the postulation of 12-h rather than 24-h period of alternations between the buildup and decay phases of $X_u(t)$, that is, the homeostatic process representing the influence of the sleep drive (3a) on the opposing wake drive (1a,1b).

The least-squares method was used to simulate seven 24-h locomotor activity curves, as illustrated in Figures 1B and 3, and seven 24-h locomotor activity curves, as illustrated in Figures 1C and 4. The ranges of variation of the parameters of the model presented in Tables 2 and 3 (for locomotor and activity curves, respectively) were not limited, with the exception of the assumption of identity of the two phase parameters of circadian modulation, t_1 and φ_0 for $\boldsymbol{X(t)}$ and $X_u(t)$, ie, for the wake and sleep processes, respectively.

https://doi.org/10.2147/NSS.S497563

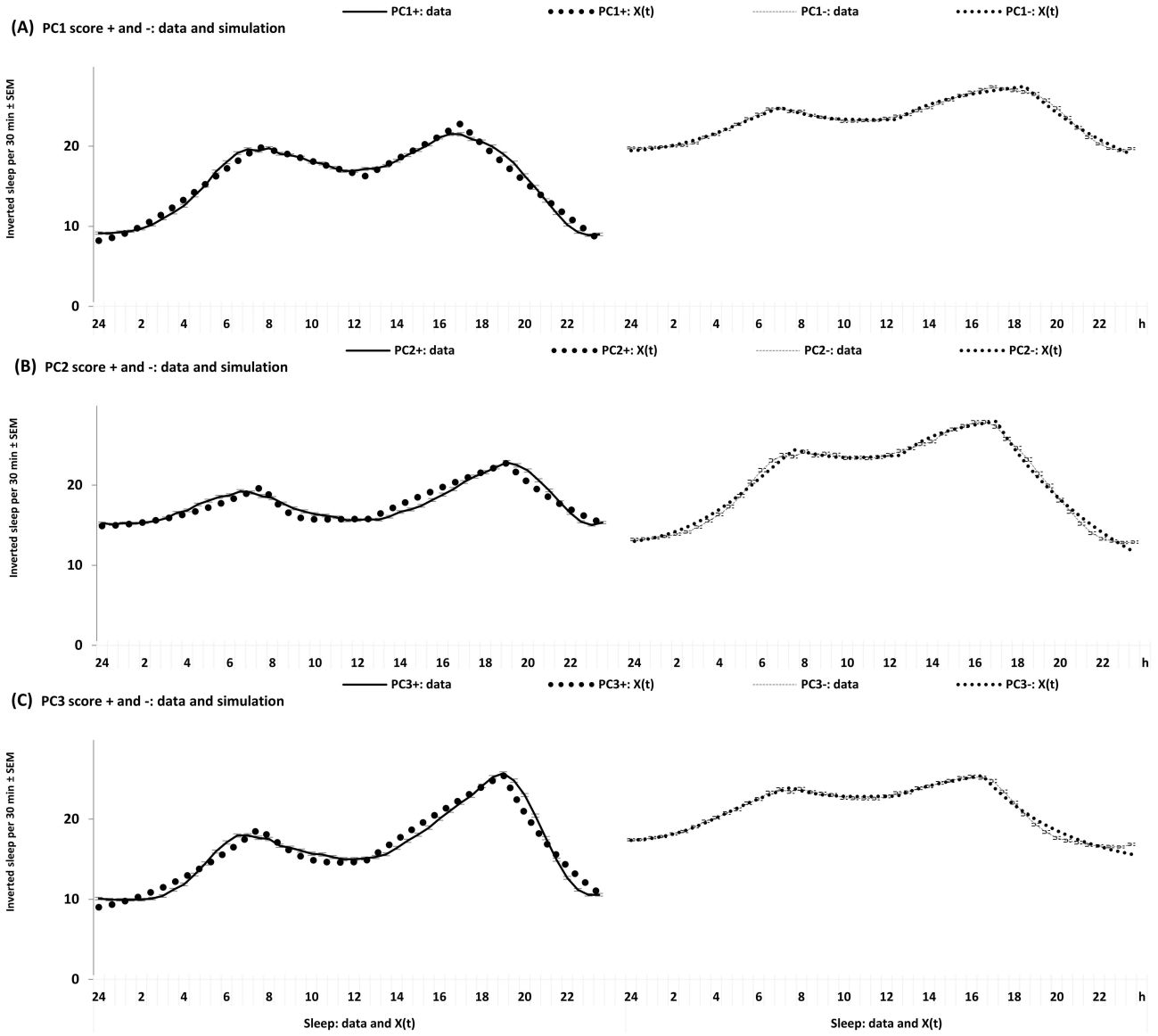

Figure 4 Simulations of sleep curves for subsamples with different principal component scores. (**A**–**C**) The 24-h sleep curves for subsamples with the dichotomized scores (above and below zero) on the 1st, 2nd, and 3rd principal components, respectively, and their simulations, *X(t)*. Left and right: 24-h curves for scores above and below zero, respectively. These sleep curves were inverted for simulation.

Results

The Typical 24-h Patterns of Locomotor Activity and Sleep

Despite the fact that the recording of locomotor activity of the vast majority of flies included in the whole sample in DD, the sample-averaged curve (Figures 1A and S1) demonstrates the persistence of an approximately 24-h locomotor rhythm with two morning and evening peaks. The times of these peaks indicated that increase in activity anticipates light-on and light-off transitions occurring during equinoxes (light between 7:30 and 19:30, respectively). It is also notable that such features of the bimodal pattern of 24-h rhythms persisted (Figures 1A and 2) despite the recordings of locomotor activity and sleep in the vast majority of flies under high temperature (29°C) that was usually combined with additional harsh conditions, such as low caloric diets or caffeinated food (Figure S2). The effects of the particular conditions on the 24-h curves were described in detail in the previous publications (Zakharenko, 2018, 2021, 2023, 2024).[19–22]

Principal component analysis of the whole sample of curves yielded three principal components that explained more than 70% of the individual variation in these curves (Table 1, upper part). Scores on the 1st, 2nd and 3rd principal

components were dichotomized to calculate the 24-h curves for the subsamples with positive and negative scores, either >0 or ≤0 (Figure 2B-D). The main features of the curves of locomotor activity (as compared with the averaged curve) are presented in Table 1 (lower part).

Notably, although the waveform of the group-averaged 24-h curves varied considerably in 12 datasets constituting the whole sample of individual curves (Figure S2), the typical bimodal pattern was demonstrated by each of the typical curves representing the subsamples with the 1st, 2nd, and 3rd principal component scores above and below or equal to zero (Figure 2B-D).

The results of principal component analysis and scoring provided a possibility to reduce the remarkable variety of the individual curves to a manageable number of such typical curves. Therefore, we simulated (Figures 1B, C, 3 and 4), in total, 14 such typical curves, the sample-averaged curves of locomotor activity and sleep (Figure 1A, left and right graph, respectively) and the subsample-averaged curves, 6 for locomotor activity and 6 for sleep (Figure 2B-D, left and right, respectively).

Simulations of the Typical 24-h Patterns

The only common feature of these six typical curves was the absence of remarkable variation in the timing of the morning peak (Table 1, lower section). Therefore, two parameters of the model, t_1 and φ_0 (initial time for buildup of activity and circadian phase, respectively), were proposed to be identical for $X(T)$ and $X_u(t)$ representing the drivers for wake and sleep, respectively (Tables 2 and 3, and Figures 1B and S1). Despite the stability of the morning peak, the phase angle between t_1 and φ_0 can be suggested to slightly vary in simulations (Tables 2 and 3).

Unlike the morning peak, the evening peak exhibited profound variability in the two pairs of curves calculated for the 2nd and 3rd principal component. In the simulations of these curves, this variation was mostly accounted for by shifting the remaining phase parameter, t_2 (initial time for decay of activity), on earlier or later clock times (Tables 2 and 3, and Figures 3 and 4).

Table 2 Parameters of the Model (1–3) Derived by Simulating Seven Curves of Locomotor Activity

		Averaged	PC1		PC2		PC3	
Parameter	**Parameter Name**		**+**	**–**	**+**	**–**	**+**	**–**
t1 and *t2*	Initial times for buildup (1a) and decay phase (1b) of activity							
t1	Buildup begins	24.00	24.00	24.00	24.00	24.00	24.00	24.00
t2	Decay begins	18.50	18.50	18.50	19.00	17.00	19.00	16.50
C(t)	Sine-form modulation (2) of parameters of buildup (1a) and decay (1b) of activity							
A	Amplitude	1.94	2.32	1.51	0.20	0.59	0.20	0.62
φ_{max}	Phase	7.08	6.74	9.03	9.97	7.27	8.53	7.99
X(t)	Inverse exponential buildup (1a) and exponential decay phase (1b) of activity							
X_d	Highest buildup	24.10	40.35	14.11	22.93	28.95	32.37	32.49
X_b	Lowest decay	9.07	16.65	4.50	13.50	3.00	7.30	8.00
X_l	Lower asymptote	−8.00	2.00	−3.73	9.75	−4.00	3.00	3.00
T_b	Constant for buildup	19.53	13.03	15.70	41.67	14.94	20.05	11.83
T_d	Constant for decay	5.99	4.10	4.50	4.10	4.10	4.10	4.10

(*Continued*)

https://doi.org/10.2147/NSS.S497563

Table 2 (Continued).

		Averaged	PC1		PC2		PC3	
Parameter	**Parameter Name**		**+**	**–**	**+**	**–**	**+**	**–**
$X_u(t)$	Inverse exponential buildup and exponential decay phase of higher asymptote (3)							
A_u	Amplitude	1.94	1.19	2.34	3.00	3.00	1.61	2.19
φ_{maxu}	Phase	7.08	6.74	9.03	9.97	7.27	8.53	7.99
X_{dl}	Highest buildup	46.05	60.19	22.81	49.42	55.28	55.39	51.53
X_{bl}	Lowest decay	20.00	25.00	8.00	22.00	22.00	22.00	22.00
X_{ll}	Lower asymptote	15.21	20.00	7.17	14.00	5.00	14.00	15.08
X_{ul}	Higher asymptote	54.97	62.5	40.0	100.0	59.3	100.0	37.04
T_{bu}	Constant for buildup	7.67	4.10	11.97	18.85	6.99	14.33	9.25
T_{du}	Constant for decay	4.00	5.14	4.10	4.10	9.36	4.10	4.29
	Normalized sum of squares							
		0.03	0.06	0.02	0.34	0.06	0.18	0.04

Notes: Parameters used for the seven simulations of the 24-h locomotor activity curve. Averaged: curve obtained by averaging individual curves (n=4263). PC1, PC2, and PC3: six curves for subsamples with dichotomized scores on the 1st, 2nd and 3rd principal components (above and below or equal to zero, +, and −, respectively). φ_{max}: clock time for the maximum sine function (suggested to be the same for the circadian modulation of $X_u(t)$ and $X(t)$), $\varphi_{max} = \varphi_{maxu}$. Normalized sum of squares: simulations of the 24-h curves performed using the least-squares method. The sum of the squared offsets was normalized by the number of offsets used in the calculation of the sum.

Table 3 Parameters of the Model (1–3) Derived by Simulating Seven Sleep Curves

		Averaged	PC1		PC2		PC3	
Parameter	**Parameter Name**		**+**	**–**	**+**	**–**	**+**	**–**
t1 and *t2*	Initial times for buildup (1a) and decay phase (1b) of activity							
t1	Buildup begins	24.00	24.00	24.00	24.00	24.00	24.00	24.00
t2	Decay begins	18.00	17.00	18.50	19.00	17.00	19.00	16.50
C(t)	Sine-form modulation (2) of parameters of buildup (1a) and decay (1b) of activity							
A	Amplitude	0.01	3.00	0.01	0.25	0.91	0.20	0.01
φ_{max}	Phase	6.89	5.42	8.40	9.81	8.96	9.97	6.46
X(t)	Inverse exponential buildup (1a) and exponential decay phase (1b) of activity							
X_d	Highest buildup	25.54	22.84	27.49	22.74	27.95	25.54	25.44
X_b	Lowest decay	15.52	8.22	19.45	14.90	13.00	9.00	17.37
X_l	Lower asymptote	−4.90	0.00	12.70	11.41	5.00	3.00	13.45
T_b	Constant for buildup	24.86	20.46	20.72	50.65	17.83	19.50	24.29
T_d	Constant for decay	12.65	6.50	5.86	4.10	4.83	4.10	4.10

(*Continued*)

Table 3 (Continued).

		Averaged	PC1		PC2		PC3	
Parameter	**Parameter Name**		**+**	**–**	**+**	**–**	**+**	**–**
$X_u(t)$	Inverse exponential buildup and exponential decay phase of higher asymptote (3)							
A_u	Amplitude	3.00	0.01	2.11	3.00	3.00	3.00	3.00
φ_{maxu}	Phase	6.89	5.42	8.40	9.81	8.96	9.97	6.46
X_{dl}	Highest buildup	45.11	39.71	38.19	49.91	44.16	39.23	42.11
X_{bl}	Lowest decay	18.35	21.08	25.02	16.00	28.53	16.99	24.40
X_{ll}	Lower asymptote	44.28	63.29	38.02	100.00	45.00	100.00	40.00
X_{ul}	Higher asymptote	20.00	18.00	23.00	22.00	21.00	20.00	21.73
T_{bu}	Constant for buildup	5.77	10.74	4.67	18.59	6.04	28.38	5.15
T_{du}	Constant for decay	5.97	4.49	4.10	3.50	5.18	4.43	5.30
	Normalized sum of squares							
		0.01	0.03	0.01	0.06	0.02	0.05	0.02

Notes: Parameters used for seven simulations of the 24-h sleep curve. See notes in Table 2.

Overall, the results of simulations (Figures 1B, C, 3, and 4) of the typical locomotor activity and sleep curves (Figures 1A and 2B-D) suggested that the assumption of two separate oscillators were not necessary to include in the model to simulate these typical curves of the locomotor activity and sleep (see the bottom line in Tables 2 and 3 for the extent of deviation of the simulated curves from the empirically obtained curves). As indicated by the results shown in Tables 2 and 3, the variation in the major features of the typical curves (Table 1, lower part) can be attributed to the variation in some of the parameters of the two homeostatic processes representing the 24-h and 12-h alternations of the drives for wake and sleep, respectively.

Discussion

To our knowledge, this is the first attempt to implicate a model with two rather than one underlying homeostatic process and with only one circadian oscillator to explain and simulate the features of bimodal 24-h rhythm of *Drosophila* locomotor activity and sleep. Since fly sleep is conventionally defined as 5 consecutive minutes of the absence of any locomotor activity (Donelson et al, 2012),[12] sleep can be simply viewed as another measure of locomotor activity. The present results of simulation of 14 typical curves of locomotor activity and sleep suggested that the postulation of more than one circadian oscillator is not necessary to explain individual variation in the bimodal 24-h rhythms of this species. The individual differences can originate from the differences in some of the parameters of the two opposite homeostatic processes, representing the 24-h variation in the drive for wake and the 12-h variation of the drive for sleep. For instance, such particular parameter of the wake homeostatic process as the timing of the switch between its two (buildup and decay) phases can explain the observations of advancing and delaying shifts of the evening peak relative to the unshifted morning peak. This specific response of the bimodal 24-h rhythm of behavior was observed in flies adjusting to the seasonal and experimental changes in photoperiod (eg, Menegazzi et al, 2020; Kauranen et al, 2012; Rieger et al, 2012; Kistenpfennig et al, 2018).[5,27–29] Further simulations applying the proposed model can be aimed on explaining the experimental results on the responses of morning and evening peaks of the *Drosophila* rhythm to different circadian periods of external (entraining) cycles (eg, Vaze et al, 2023).[30]

The classical two-process model (Daan et al, 1984; Abhilash, Shafer, 2024; Skeldon, Dijk, 2024)[8,10,11] appears to be too simple to account for such differences in responses of morning and evening peaks to the changes in duration and period of the external lighting condition. On the other hand, it is not necessary to assume the involvement of more than one oscillator (Pittendrigh, Daan, 1976; Yoshii et al, 2023)[3,7] in this differential response of the morning and evening peaks. The present results of simulations of 14 typical curves suggested that, for a purpose of their parsimonious

https://doi.org/10.2147/NSS.S497563

description and explanation, a model with just three components might be optimal. Our model allowed not only the fitting a variety of patterns of fly's locomotor activity and sleep, but also the explanation of the underlying differences between them in terms of the two opposing processes representing the drives for wake and sleep. In this respect, it appears to be more suitable for generalization of the underlying regulatory mechanisms over various animal species than other three-component models postulate a human-specific processes, such as sleep inertia (Achermann, Borbély, 1994; Akerstedt, Folkard, 1997)[13,14] or the wake- and sleep-promoting areas in the brain (Phillips et al, 2013).[16]

Previously, we applied principal component analysis to the 24-h curves of *Drosophila* activity and sleep to demonstrate that the curves of parent strains contribute approximately equally to the curves of their hybrids, that is, additive genetic effects (Zakharenko et al, 2024).[20] Here, we demonstrated for the first time that this methodology can be also applied to determine typical 24-h curves from a sample of many individual curves that can be profoundly variable in their waveforms because these curves were obtained under rather harsh experimental and environmental conditions. In addition, this approach allows for a quantitative representation of each individual-averaged or group-averaged curve using only three principal component scores. The application of this approach to 12 datasets suggested significant differences between just three group-averaged scores (Figure S3) that were in line with the differences revealed by a traditional statistical analysis of the curves consisting of as many as 48 time points (eg, shown in Tables S3–S5).

Notably, the extent of variation in the 24-h patterns of locomotor activity and sleep uncovered by applying principal component scoring of individual patterns was remarkably smaller (Figure 2B-D) compared to the patterns observed in each of 12 experiments, especially in those flies that were at old age and/or exposed to harsh environment, such as high temperature combined with low caloric diets and/or caffeinated food (Figure S2; see Zakharenko, 2018, 2021, 2023, 2024,[19–22] for more details). The results suggested that the 24-h rhythms with two peaks occurring near the expected times of sunrise and sunset persisted in each of such typical 24-h patterns of locomotor activity and sleep.

Conclusion

In this study, we examined whether a model postulating circadian modulation of the buildup and decay phases of two opposing homeostatic processes can be applied to simulate the bimodal 24-h rhythm of locomotor activity and sleep in *Drosophila melanogaster*. The results suggest that the bimodal curves can be simulated by proposing the variation of some of the parameters of these two underlying homeostatic processes that can represent the 24-h variation in the drive for wakefulness and the 12-h variation in the opposing drive for sleep. It was not necessary to postulate more than one circadian modulator of these processes.

Abbreviations

DAMS, Drosophila Activity Monitoring System; PC, principal component; LD, light–dark cycle.

Data Sharing Statement

All data are available from the last author on reasonable request.

Funding

The work of L.P.Z. and D.V.P. was supported by the Budget Project #FWNR-2022-0019 from the Ministry of Science and Higher Education of the Russian Federation, Russia.

Disclosure

The authors report no conflicts of interest in this work.

References

1. Aschoff J. Circadian activity pattern with two peaks. *Ecology*. 1966;47:657–662. doi:10.2307/1933949
2. Lazopulo A, Syed S. A computational method to quantify fly circadian activity. *J Vis Exp*. 2017;(128):55977. doi:10.3791/55977
3. Pittendrigh CS, Daan S. A functional analysis of circadian pacemakers in nocturnal rodents. V. Pacemaker structure: a clock for all seasons. *J Comp Physiol*. 1976;106:333–355. doi:10.1007/BF01417860
4. Peschel N, Helfrich-Förster C. Setting the clock–by nature: circadian rhythm in the fruitfly *Drosophila melanogaster*. *FEBS Lett*. 2011;585 (10):1435–1442. doi:10.1016/j.febslet.2011.02.028

5. Menegazzi P, Beer K, Grebler V, Schlichting M, Schubert FK, Helfrich-Förster C. A functional clock within the main morning and evening neurons of *D. melanogaste*r is not sufficient for wild-type locomotor activity under changing day length. *Front Physiol*. 2020;11:229. doi:10.3389/fphys.2020.00229
6. Grima B, Chélot E, Xia R, Rouyer F. Morning and evening peaks of activity rely on different clock neurons of the *Drosophila* brain. *Nature*. 2004;431(7010):869–873. doi:10.1038/nature02935
7. Yoshii T, Saito A, Yokosako T. A four-oscillator model of seasonally adapted morning and evening activities in *Drosophila melanogaster*.. *J Comp Physiol a Neuroethol Sens Neural Behav Physiol*. 2023;210:527–534. doi:10.1007/s00359-023-01639-5
8. Borbély AA. A two process model of sleep regulation. *Hum Neurobiol*. 1982;1:195–204.
9. Daan S, Beersma DGM, Borbély AA. Timing of human sleep: recovery process gated by a circadian pacemaker. *Am J Physiol Regul Integr Comp Physiol*. 1984;246:R161–R178. doi:10.1152/ajpregu.1984.246.2.R161
10. Abhilash L, Shafer OT. A two-process model of *Drosophila* sleep reveals an inter-dependence between circadian clock speed and the rate of sleep pressure decay. *Sleep*. 2024;47(2):zsad277. doi:10.1093/sleep/zsad277
11. Skeldon AC, Dijk DJ. Modeling *Drosophila* sleep: fly in the sky? *Sleep*. 2024;47(2):zsad309. doi:10.1093/sleep/zsad309
12. Donelson NC, Kim EZ, Slawson JB, Vecsey CG, Huber R, Griffith LC. High-resolution positional tracking for long-term analysis of *drosophila* sleep and locomotion using the "tracker program. PLoS ONE. 2012;7:e37250. doi:10.1371/journal.pone.0037250
13. Achermann P, Borbély AA. Simulation of daytime vigilance by the additive interaction of a homeostatic and a circadian process. *Biol Cybern*. 1994;71(2):115–121. doi:10.1007/BF00197314
14. Akerstedt T, Folkard S. The three-process model of alertness and its extension to performance, sleep latency, and sleep length. *Chronobiol Int*. 1997;14(2):115–123. doi:10.3109/07420529709001149
15. Jewett ME, Forger DB, Kronauer RE. Revised limit cycle oscillator model of human circadian pacemaker. *J Biol Rhythms*. 1999;14(6):493–499. doi:10.1177/074873049901400608
16. Phillips AJ, Fulcher BD, Robinson PA, Klerman EB. Mammalian rest/activity patterns explained by physiologically based modeling. *PLoS Comput Biol*. 2013;9(9):e1003213. doi:10.1371/journal.pcbi.1003213
17. Putilov AA, Donskaya OG, Verevkin EG. Phase difference between chronotypes in self-reported maximum of alertness rhythm: an EEG predictor and a model-based explanation. *J Psychophysiol*. 2014;28:242–256. doi:10.1027/0269-8803/a000116
18. Putilov AA, Donskaya OG, Verevkin EG. How many diurnal types are there? A search for two further "bird species". *Pers Individ Dif*. 2015;72:12–15. doi:10.1016/j.paid.2014.08.003
19. Zakharenko LP, Petrovskii DV, Putilov AA. Larks, owls, swifts, and woodcocks among fruit flies: differential responses of four heritable chronotypes to long and hot summer days. *Nat Sci Sleep*. 2018;10:181–191. doi:10.2147/NSS.S168905
20. Zakharenko LP, Petrovskii DV, Dorogova NV, Putilov AA. Association between the effects of high temperature on fertility and sleep in female intra-specific hybrids of *Drosophila melanogaster*. *Insects*. 2021;12(4):336. doi:10.3390/insects12040336
21. Zakharenko LP, Bobrovskikh MA, Gruntenko NE, Petrovskii DV, Verevkin EG, Putilov AA. Two old wild-type strains of *Drosophila melanogaster* can serve as an animal model of faster and slower aging processes. *Insects*. 2024;15(5):329. doi:10.3390/insects15050329
22. Zakharenko LP, Petrovskii DV, Bobrovskikh MA, et al. Motus vita Est: fruit flies need to be more active and sleep less to adapt to either a longer or harder life. *Clocks Sleep*. 2023;5(1):98–115. doi:10.3390/clockssleep5010011
23. Pfeiffenberger C, Lear BC, Keegan KP, Allada R. Locomotor activity level monitoring using the drosophila activity monitoring (DAM) system: figure 1. *Cold Spring Harb Protoc*. 2010;2010:pdb–prot5518.
24. Putilov AA. The timing of sleep modelling: circadian modulation of the homeostatic process. *Biol Rhythm Res*. 1995;26:1–19. doi:10.1080/09291019509360320
25. Edgar DM, Dement WC, Fuller CA. Effect of SCN lesions on sleep in squirrel monkeys: evidence for opponent processes in sleep-wake regulation. *J Neurosci*. 1993;13(3):1065–1079. doi:10.1523/JNEUROSCI.13-03-01065.1993
26. Dijk DJ, Czeisler CA. Contribution of the circadian pacemaker and the sleep homeostat to sleep propensity, sleep structure, electroencephalographic slow waves, and sleep spindle activity in humans. *J Neurosci*. 1995;15(5 Pt 1):3526–3538. doi:10.1523/JNEUROSCI.15-05-03526.1995
27. Kauranen H, Menegazzi P, Costa R, Helfrich-Förster C, Kankainen A, Hoikkala A. Flies in the north: locomotor behavior and clock neuron organization of *Drosophila Montana*. *J Biol Rhythms*. 2012;27(5):377–387. doi:10.1177/0748730412455916
28. Rieger D, Peschel N, Dusik V, Glotz S, Helfrich-Förster C. The ability to entrain to long photoperiods differs between 3 *Drosophila melanogaster* wild-type strains and is modified by twilight simulation. *J Biol Rhythms*. 2012;27(1):37–47. doi:10.1177/0748730411420246
29. Kistenpfennig C, Nakayama M, Nihara R, Tomioka K, Helfrich-Förster C, Yoshii T. A tug-of-war between cryptochrome and the visual system allows the adaptation of evening activity to long photoperiods in *Drosophila melanogaster*. *J Biol Rhythms*. 2018;33(1):24–34. doi:10.1177/0748730417738612
30. Vaze KM, Manoli G, Helfrich-Förster C. *Drosophila ezoana* uses morning and evening oscillators to adjust its rhythmic activity to different daylengths but only the morning oscillator to measure night length for photoperiodic responses.. *J Comp Physiol a Neuroethol Sens Neural Behav Physiol*. 2023;210:535–548. doi:10.1007/s00359-023-01646-6